v1: 30 December 2023

Research Article

Optimized Material Removal and Tool Wear Rates in Milling API 5ST TS-90 Alloy: AI-Driven Optimization and Modelling with ANN, ANFIS, and RSM

Peer-approved: 30 December 2023

Qeios, Vol. 5 (2023)
ISSN: 2632-3834

Chinedum Mgbemena[1], Shadrach Osokam Onyegu[2]

1. Department of Mechanical Engineering, Federal University of Petroleum Resources, Nigeria; 2. Federal University of Petroleum Resources, Nigeria

One of the performance measures and responses in manufacturing is the optimization of the Material Removal Rate (MRR) and Tool Wear Rate (TWR). This study used the response surface method (RSM) and AI-based models of artificial neural networks (ANNs) and adaptive neuro-fuzzy inference systems (ANFISs) to model and optimize the MRR and TWR for milling API 5ST TS-90 alloys. A ZX6350C milling machine was used to conduct twenty (20) experimental runs using a 10 mm HSS end-mill cutter. The experiment was designed using Central Composite Design (CCD) in Design Expert 14 software. RSM, ANN, and ANFIS models were applied in the predictive modelling of the milling process with a coefficient of determination above 0.85. Comparatively, ANFIS and RSM were marginally better than ANN in the predicted MRR for the milling process. The ANFIS and RSM were slightly better than ANN in the predicted TWR for the milling operation. Generally, ANFIS showed a better predictive capability than RSM and ANN for both MRR and TWR. The optimum process milling parameters for the alloy were a 720-rpm spindle speed, 24 mm/min feed rate and 0.979 mm depth of cut to achieve an optimized predicted MRR of 1272.163 mm3/min and TWR of 0.781 mm/min. The optimum milling process was validated at the suggested experimental conditions by carrying out the milling experiment at those conditions, and the results of 1270.05 mm3/min for MRR and 0.77 mm/min for TWR showed a close correlation between the predicted and validated optimum. The optimum milling parameters from this study would enhance production at reduced tooling costs associated with tool wear.

Corresponding author: Chinedum Mgbemena, mgbemena.ogonna@fupre.edu.ng

1. Introduction

In recent times, the sole aim of every manufacturing industry has been to increase productivity most cost-effectively without impacting product quality, which inadvertently reduces its acceptability in the market. To survive the ever-evolving market and stiff competition, manufacturers rely heavily on productivity and associated costs. Recent improvements in engineering design have been a primary driver behind technical advancements in practically all engineering domains. In the metal-cutting industry, manufacturers are continuously exploring the advancement of appropriate machining techniques that can guarantee highly accurate components while minimizing costs, thereby accelerating, and automating various machining operations (Sada & Ikpeseni, 2021). The API 5ST TS-90 Alloy to be studied in this research work is a low-carbon alloy steel with an enormous application in the Oil and Gas sector, especially for the manufacturing of well intervention equipment used in Matrix Acidization, Scale Treatment, Tubing Wash, Sand Clean-out, Nitrogen

 doi.org/10.32388/GEGPL7.2

Lift, Cementing via coil, Fishing, etc. Material Removal Rate and Tool Wear Rate are key factors in all machining operations, and they have significant cost implications in milling activities (Mgbemena et al., 2016).

Several industrial applications of milling processes show that the control and optimization of both material removal and tool wear rates are among the most important performance measures and responses in manufacturing (Himanshu et al., 2019). Utilizing machining procedures, cutting tool life and wear can be increased to lower part production costs (Mohsen & Mohammed, 2022). Manufacturing engineering has long struggled with the age-old challenge of monitoring the machining process. Users of cutting tools cannot afford to disregard the ongoing developments and changes in the science of tool material. To prevent the item being machined from failing to meet the stipulated tolerance as a result of using the worn-out tool, the tool should be withdrawn and replaced well before it wears out completely. This might also lead to a task with poor surface quality, increasing production costs overall owing to an increase in rework and scrap (Liu et al., 2023, Shrikrishna et al., 2018). Therefore, to increase productivity by reducing tooling and machining costs, the manufacturing engineer should be able to determine optimum milling process parameters. The overall control and optimization of a manufacturing process is the economic aim alongside the technical requirements needed (Bouzid et al., 2020). The adoption and use of statistical methods and artificial intelligence (AI)-based models such as artificial neural networks (ANNs) and other hybrid models such as the adaptive neuro-fuzzy inference system (ANFIS), which combines ANN and fuzzy logic, are currently paving the way towards achieving technical and economic milestones in efficient process predetermination (Banza et al., 2023; Daniel et al., 2023; Asadi et al., 2019; Singh et al., 2019; Chabbi et al., 2017; Okwu and Adetunji, 2018).

High productivity, good surface finish and optimum tool life are of great relevance in manufacturing. To be competitive in a fast-paced marketplace, the economy of machining, not to the detriment of quality, comes into play. The selection of milling parameters is highly dependent on the experience of the machinist or perhaps on machining data obtained from machine tool handbooks. Machining process parameters obtained from these sources are most likely conservative and riddled with several uncertainties and may not yield the desired quality and output; hence, it is deemed fit to develop a novel approach in obtaining adjusted process design parameters from predicted models using artificial intelligence techniques for the investigation and solution of milling optimization problems. In this work, artificial intelligence tools in the form of an artificial neural network (ANN), adaptive neuro-fuzzy inference system (ANFIS) and response surface method (RSM), a statistical model, were implemented in modelling and optimizing material removal and tool wear rates in milling API 5ST TS-90 Alloy to reduce the tooling cost and maximize production. One of the most important and traditional shaping techniques for the economically viable fabrication of machine components is material removal. Fast and accurate machining issues have received much attention recently in the manufacturing sector due to the widespread use of engineering materials and alloy steels with high hardness in industry. Thus, fast-cutting tool failure causes the integrity of the work piece's surface to be compromised, geometric tolerances to be lost, and machining times to increase. The increase in machining time is caused by downtime as a result of changing and resetting cutting tools, as well as a loss in tool life, which eventually results in increases in unit cost (Kundrak et al., 2018; Coppini & dos Santos, 2015).

A review of the literature on material removal rates (MRRs) and tool wear rates (TWRs) in milling has been reported by different researchers by using regression and other mathematical tools to optimize cutting parameters and a few applied intelligent models, such as RSM, ANN and ANFIS, in their work. However, the predictive modelling of MRR and TWR in milling using combined intelligent models such as ANFIS, ANN, and RSM has not been reported. The use of ANFIS in modelling the optimization of machining parameters in milling processes was reported by Shukry et al. (2018) and Sandeep et al. (2019) for MRR, while ANN was reported by Salimiasi and Özdemir (2016) and Bagga et al. (2021) for TWR, and RSM was reported by Zhang et al. (2019) for MRR, Wickramarachchi et al. (2021) for TWR and Hsu & Ngayen (2017) for MRR. Therefore, this work will provide a detailed analysis of the use of ANFIS, ANN, and RSM in the predictive modelling of material removal and tool wear rates in milling API 5ST TS 90 alloy. Furthermore, a comparative analysis of the three models, which have not been reported elsewhere, was investigated, and reported in this work.

2. Materials and Methods

The study was conducted using API 5ST TS-90 hollow cylindrical alloy steel with outer and inner diameters of 38.1 mm and 31.75 mm, respectively, and a 50 mm length as a specimen. The chemical composition and mechanical properties of the specimen are shown in Tables 1 and 2. The cutting tool used for the milling operation is a SWT 10 X 10 four-flute HSS tool with a hardness of 67 HRB. The chosen HSS cutter can withstand higher feed rates due to its high level of hardness. A ZX6350C milling machine with a variable spindle speed of 1750 rpm and a 1.5 kW main motor drive was used for the milling operation. The specimen was cleaned by removing approximately 0.2 mm of the top surface to eliminate surface defects, and it was

properly mounted on the milling machine by using a rigid machine vice to avoid wobbling. The detailed specifications of the milling machine are captured in Table 3. The experiment was carried out under dry machining conditions.

doi.org/10.32388/GEGPL7.2

Content %										
C	Mn	P	S	Si	Cr	Mo	Ni	Cu	Nb	Ti
0.14	0.76	0.02	0.001	0.33	0.59	0.15	0.14	0.30	0.015	0.02

Table 1. Chemical composition of API 5ST TS-90 alloy

doi.org/10.32388/GEGPL7.2

Mechanical property			
Yield strength (N/m^2)	Tensile strength (N/m^2)	Elongation (%)	Hardness
6.8E8	7.4E8	22.0	97HRB

Table 2. Mechanical properties of API 5ST TS-90 alloy

doi.org/10.32388/GEGPL7.2

Specification	ZX6350C
Distance from spindle nose to table	90-400 mm
Maximum vertical milling diameter	25 mm
Maximum end milling width	100 mm
Spindle speed range	1750rpm
Table size	1120 x 280
Table travel	600 mm x 230 mm
Main motor	1.5Kw
Spindle travel	120 mm
Overall dimension	1352 mm x 1285 mm x 2130 mm
Gross weight	1350 kg

Table 3. ZX6350C milling machine specification.

2.1. Research Design

The method adopted in this research work was a mix of both experimental and software-aided design methods to model and optimize the MRR and TWR of API 5ST TS-90 alloy steel during an end-milling operation. The factors and their associated effects studied in this research are the depth of cut (mm), spindle speed (rpm) and feed rate (mm/min) on the material removal rate (MRR) and tool wear rate (TWR) in an end milling operation. Central composite design (CCD) was used with the aid of Design Expert Software to develop a three-level experimental matrix made up of twenty (20) experimental runs based on input parameters (depth of cut, feed rate and spindle speed) and their respective ranges. The experiment focused on MRR and TWR as responses.

The experiment was carried out by rigidly fixing the workpiece on a vice on the bed of the ZX6350C milling machine; thereafter, the milling parameters were set, and the machine was powered on. The temperature of the workpiece was measured after each machining operation by using an optical pyrometer as well as the weight of the workpiece before and after experimentation using a sensitive weighing scale; cutting tool length was also measured before and after every cut by using a digital Vernier calliper, and the machining time was also captured. The experimentation was carried out under dry milling conditions. The weight of the sample was measured before and after each phase of the milling test operation. Similarly, the running time for the tests was recorded to compute the material removal rate. The material removal rate was calculated using measurable data, such as changes in material weight and machining time. The tool wear rate was also obtained from measurable data, that is, changes in the length of the cutting edge with machining time.

Figure 1. ZX6350C milling machine and workpiece.

In milling processes, the metal removal rate (MRR) is the volume or weight of material removed per unit of time in mm3/min or g/min. Materials are removed from the workpiece in the form of chips for each revolution of the mill cutter while the workpiece is fed into it. The MRR is stated mathematically as (Parthasarathi et al., 2022; Mgbemena et al., 2016):

$$MRR = (W_i - W_f)/\rho t \tag{1}$$

The MRR can also be obtained by calculating the weight of material removed per unit time(g/min), as shown in equation 2 below (Shagwira et al., 2021):

$$MRR = (W_i - W_f)/t \tag{2}$$

where $MRR(\mathrm{mm}^3/\mathrm{min}$ or $\mathrm{g}/\mathrm{min})$ is the material removal rate, $W_i(g)$ is the initial weight of the work piece before milling, $W_f(g)$ is the weight of the workpiece after milling, and $\rho(g/\mathrm{mm}^3)$ is the density of the steel alloy. For the steel alloy used in this study, the density is $0.0078(g/\mathrm{mm}^3)$.

The tool wear rate (TWR) is seen as the amount of volume loss of cutting tool material on the contact surface caused by interactions between the cutting tool and work piece. It is stated mathematically as shown below (Kumar et al., 2016; Mgbemena et al., 2016):

$$TWR = (L_i - L_f)/t \tag{3}$$

where $TWR(mm/min)$ is the tool wear rate, $L_i(mm)$ is the length of the cutting tool before milling, $L_f(mm)$ is the length of the cutting tool after milling and $t(min)$ is the time taken for each experimental run.

Data collection for the milling operation was carried out in real time during the experiments. Data for the respective responses were recorded twice, and averages were taken for better accuracy. A digital pyrometer was used to measure the workpiece temperature before and after each experimental run. A sensitive weighing scale was used to measure the weight of the specimen before and after the milling operation. The length of the mill cutter was also recorded before and after every experimental run using a digital Vernier calliper, while a stopwatch was used to measure the machining time. Table 4 captures the responses (MRR and TWR) from the different input parameters in the milling process.

2.2. Analytical Tool/Method of Data Analysis

In this research, the key analytical tools from statistics and artificial intelligence used in this study are the response surface method (RSM), analysis of variance (ANOVA), artificial neural network (ANN) and adaptive neuro-fuzzy inference system (ANFIS).

Runs	Spindle speed (RPM)	Feed rate (mm/min)	DOC (mm)	MRR (mm^3/min)	TWR (mm/min)
1	505	44.5	0.75	923.08	0.88
2	720	44.5	0.75	1230.77	1.04
3	505	44.5	0.75	923.08	0.96
4	720	24	0.5	153.85	0.44
5	290	24	1	1128.21	0.72
6	505	44.5	1	1179.49	1.56
7	720	65	1	1589.74	2.08
8	505	44.5	0.5	256.41	0.64
9	720	24	1	1282.05	0.80
10	290	44.5	0.75	1076.92	0.88
11	505	44.5	0.75	923.08	0.96
12	505	44.5	0.75	923.08	1.00
13	720	65	0.5	717.95	0.84
14	290	24	0.5	102.56	0.28
15	505	44.5	0.75	923.08	0.96
16	505	24	0.75	666.67	0.48
17	290	65	1	1230.77	1.84
18	505	65	0.75	1000.00	1.80
19	290	65	0.5	512.82	0.84
20	505	44.5	0.75	923.08	0.92

Table 4. Results of DOE for API 5ST TS-90 alloy end milling operations

2.2.1. Response surface Method (RSM)

Response surface methodology (RSM) modelling of the material removal rate (MRR) and tool wear rate (TWR) was investigated using central composite design (CCD). This was done to determine the best conditions for optimum milling of API 5ST TS-90 Alloy. Equally, this helps to examine the interactive effects of the three important factors or parameters. The factors considered for the machining operation were spindle speed (rpm), depth of cut (mm) and feed rate (mm/min). These were the independent variables, whereas the dependent variables or responses were the material removal rate (mm^3/min) and the tool wear rate (mm/min). The RSM-CCD method used feed rate, depth of cut, and spindle speed as independent factors and material removal rate and tool wear rate as dependent variables, which are seen as responses. The CCD is a five-level experimental design with two factorial levels (+1 and -1), two axial levels (+α and -α), and one centre level (0). However, a face-centered method was utilized, which resulted in three (3)-level experimental designs; as a result, the independent variables were varied at each of the three (3) levels. Equation 4 was used to calculate the coded values of the process parameters:

$$N_i = (X_i - X_o)/\Delta X \quad (4)$$

where N_i is the coded value of the i^{th} variable, $X_i$is the real value of the i^{th} test variable, $X_o$is the real value of the i^{th} test variable at the center point, and ΔX is the step change of the variable. The three factor levels of the independent variables in terms of the actual factors are given in Table 5.

Parameters	Level		
	Low level (-1)	Medium level (0)	High level (+1)
Spindle speed (rpm)	290	505	720
Feed rate (mm/min)	24	44.5	65
Depth of cut (mm)	0.5	0.75	1

Table 5. Factor levels of independent variables for API 5ST TS-90 end milling

Equation 5 can be used to calculate the total number of experimental design runs, according to Abbas (2013) and Arulkumar et al. (2011):

$$N = 2^n + 2n + n_c \quad (5)$$

where N represents the number of experimental design runs and n is the number of input factors. 2^n, $2n$ and n_c represent the factorial points, axial points, and center points, respectively. In the design, 8 factorial points, 6 axial points, and 6 center points give a total of twenty (20) experimental data points. Twenty (20) data sets were used in the RSM analysis. All trials were carried out in duplicate, and the averages were calculated. The center points aided in lowering the experimental error, the axial points ensured the design of the experiment's rotation ability, and the factorial points demonstrated equal changes between low and high values (Sahu et al., 2010). By doing the experiment at random, systematic error was removed. The experimental design and RSM-CCD analysis of the machining process were carried out using Design Expert (version 13) software.

The relationship between the estimated response (Y) and the independent variables is expressed in equation 6 (Sidda et al., 2011):

$$Y = f(x_1, x_2, x_3 \ldots\ldots x_k) + \varepsilon \quad (6)$$

where $x_1, x_2, x_3 \ldots\ldots x_k$ are the independent variables; ε is the error term; and k refers to the number of independent variables.

A pure quadratic model, which is a second-order polynomial, was used to describe the relationship between the responses and the independent variables as given in equation 7.

$$Y = \beta_0 + \sum_{i=1}^{k} \beta_i X_i \ldots\ldots + \ldots \sum_{i=1}^{k} \beta_{ii} X_i^2 \ldots + \cdots \sum_{i=1}^{k-1} \sum_{j=1}^{k} \beta_{ij} X_i X_j \quad (7)$$

where Y is the estimated response; β_0 is the model constant coefficient; and β_i, β_{ii}, and β_{ij} represent coefficients obtained from the polynomial equation for the linear, quadratic, and cross products of X_i , $X_i^2$and $X_i X_j$, respectively.

Multivariate regression analysis was performed using the empirical model in Equation 7 to provide the entire quadratic model in Equation 8, which was used to model the MRR and TWR.

doi.org/10.32388/GEGPL7.2

$$Y = \beta_0 + \beta_1 X_1 + \beta_2 X_2 + \beta_3 X_3 + \beta_1 1 X_1^2 + \beta_2 2 X_2^2 + \beta_3 3 X_3^2 + \beta_1 2 X_1 X_2 + \beta_1 3 X_1 X_2 + \beta_2 3 X_2 X_3 + \varepsilon \quad (8)$$

The coefficient of determination (R^2) and the ANOVA p value were used to assess the model's acceptability.

2.2.2. Artificial Neural Network (ANN)

The artificial neural network (ANN) was explored by modelling and assessing the prediction of MRR and TWR in the milling process using the Neural Network Toolbox of MATLAB R2022b (The Mathworks Inc.). The weighted inputs that come as each neuron are processed via a nonlinear activation function to create an output signal, which is inspired by real neurons (Thike et al., 2020). The model was created using the back-propagation technique, which is one of the most often used learning algorithms in ANNs. The ANN modelling made use of the twenty data sets utilized in the RSM modelling. The ANN design, according to Nazerian et al. (2018), may be effectively modelled utilizing RSM-produced experimental data.

The ANN architecture used in this study was 3-h-2, which translates to three input neurons (representing spindle speed, feed rate, and depth of cut), an unknown number of neurons in the hidden layer, and two output neurons (representing material removal rate and tool wear rate). An iterative technique was used to determine the optimal number of neurons in the hidden layer. This was done to minimize overfitting and a decrease in the convergence rate caused by a high number of neurons or a small number of neurons, respectively. The back propagation model used the Levenberg-Marquadt algorithm; therefore, the trainlm training function was used, as well as the method of gradient descent to minimize the network's sum of square errors (MSE) (Ohale et al., 2017; Mourabet et al., 2014).

The error back propagation training approach uses weight updates to reduce the sum of squared errors for the k-number of output neurons, as seen in equation 9 (Datta et al., 2010).

$$E = 1/2 \sum_{k=1}^{K} \left(d_{kp} - o_{kp}\right)^2 \quad (9)$$

where d_kp is the desired output for the P_{th} pattern. The weight, w, of the links, as seen in equation 10;

$$w_{ji(n+1)} = w_{ji(n)} + \cap \delta_{pj} o_{pi} + \alpha \Delta w_{ji(n)} \quad (10)$$

where n is the learning step, $\cap$is the learning rate, $\alpha$is the momentum constant and $\delta_p j$ is the error for the input/output layers.

$$\delta_{pk} = \left(d_{kp} - o_{kp}\right)\left(1 - o_{kp}\right),\ k = 1, 2, \ldots K \quad (11)$$

$$\delta_{p_j} = o_{p_j}\left(1 - o_{pj}\right) \sum \delta_{pk} w_{kj},\ j = 1, 2 \ldots J \quad (12)$$

where j is the number of neurons in the hidden layers. All links are given modest random weight values to begin the training process. The input and output patterns are sequential, with the weights updated each time. Equation 13 is used to determine the mean square error (MSE) at the conclusion of each epoch attributable to all patterns.

$$MSE = \frac{1}{NP} \sum_{p=1}^{P} \sum_{k=1}^{K} \left(d_{kp} - o_{kp}\right)^2 \quad (13)$$

where NP is the number of training patterns. When the needed MSE or maximum number of epochs is reached, the training process will be ended.

The metrics for measuring the performance of the network are the minimum mean square error (MSE) and correlation coefficient (R) (Lotfan et al., 2016), as given in equations 13 and 14.

$$R = \left(\frac{\sum_{i=1}^{n} \left(v_{pre,i} - v_{pre}\right)\left(v_{\exp,i} - v_{\exp}\right)}{\sqrt{\sum_{i=1}^{n} \left(V_{\text{pre},i} - v_{\text{pre}}\right)^2 \sum_{i=1}^{n} \left(V_{\exp,i} - v_{\exp}\right)^2}} \right) \quad (14)$$

where Vpre_i and Vexp_i represent the predicted and experimental outputs, respectively, and n is the number of paired inputs or outputs.

The predictive ability of an ANN is carried out by altering the weights and biases (learning) in a network to capture the linear and nonlinear structure of the input while keeping an acceptable error limit. The weights are iteratively modified until the network produces the smallest error for each input and output data set. This is made achievable by using the right network architecture, training methods, and hyperparameters (Long et al., 2020).

Approximately 70% of the data sets were utilized for training, 15% for validation, and the remaining 15% for testing. The training data set was used to investigate the link between the network's input and output parameters. The validation data set facilitated network generalization, but the testing data set improved network predictability. More data sets assigned to training generally decrease the processing time while strengthening the model (Onu et al., 2020). Three alternative training methods, activation functions, and a number of neurons ranging from 2 to 25 were chosen for executing the network's training, validation, and testing to discover the best suitable for the machining process (Sada, 2021). The network error was examined for validation on a regular basis while the training process proceeded to initiate an early stopping strategy (Haykin, 2008).

2.2.3. Adaptive Neuro-Fuzzy Inference System (ANFIS)

The adaptive neuro-fuzzy inference system (ANFIS) is a sophisticated artificial intelligence (AI) technique that consists mostly of artificial neural networks (ANNs) supported by fuzzy logic (FL) and is utilized in the modelling of complex and/or complicated nonlinear systems (Gonzalez et al., 2020). The ANFIS model of the milling procedure was analysed using MATLAB 2022b (Fuzzy Logic ANFIS Toolbox). ANFIS is an artificial intelligence (AI) approach that combines adaptive neural network (ANN) rules and fuzzy logic (FL) theories within an adaptive network architecture to build a logical link between inputs and outputs (Sada and Ikpeseni, 2021). The ANFIS toolbox generates a fuzzy inference system (FIS) whose membership structure or parameters may be changed using either a back-propagation approach alone or in conjunction with a least-squares method. The ANN procedure, on the other hand, builds the ANFIS FIS model, which is used to learn or train data. To create an inference system, five different layers are used: the fuzzy layer, the product layer, the normalized layer, the defuzzy layer, and the total output layer, each of which consists of different nodes represented by squares and circles that permit factors to be changed and fixed, respectively. The first layer has numerous membership functions (MFs) that turn numerical input data into fuzzy inputs. The output of each node is calculated using equations 15 and 16, with O_{ij} representing the output and $\cup_{xi}$ and $\cup_{yi-2}$ representing the first layer membership functions (Mathur et al., 2016).

$$O_{1i} = \mathrm{U}_x, (x), \quad i = 1, 2 \quad (15)$$
$$O_{1i} = \mathrm{U}_x, (y), \quad i = 3, 4 \quad (16)$$

The network's second layer was based on the Takagi-Sugeno inference system, which was guided by the IF-THEN rule, as shown in equations 17 and 18 (Ying and Pan, 2008).

Rule 1: if d is A_1, V is B_1 and Fr is C_1, then

$$f_1 = x_1 d + y_1 V + z_1 Fr + u_1 \quad (17)$$

Rule 2: if d is A_2, V is B_2 and Fr is C_2, then

$$f_2 = x_2 d + y_2 V + z_2 Fr + u_2 \quad (18)$$

where d, V and Fr are the inputs representing the depth of cut (mm), spindle speed (rpm) and feed rate (mm/min), respectively; f is the output function (MRR and TWR); A_1, B_1, C_1, A_2, B_2 and C_2 are the language indicators; x_1, y_1, z_1, x_2, y_2, z_2, u_1 and u_2 are coefficients of the output functions; and f_1 and f_2 are first-degree polynomials.

Using the fuzzy subset as an algebraic multiplication, the fuzzy rules are produced by multiplying the first layer's output signals, as represented by Equation 19 (Jang et al., 1998).

$$O_{2i} = \cup A(x) \cup \beta(x), i = 1, \ldots\ldots, 4, j, k = 1, 2 \quad (19)$$

The efficacy of the second layer outputs ω̃ is determined at the third layer by normalizing them to produce an appropriate weight coefficient provided by Equation 20.

$$O_{3i} = \tilde{\omega}_i = \frac{w_i}{\sum_i wj}, i = 1, \ldots\ldots\ldots, 4 \quad (20)$$

In the 4^{th} layer, after obtaining the weight coefficients from the 3^{rd} layer, the influence of each component of the system's output is estimated using fuzzy rules, as shown in Equation 21.

$$O_i^4 = \tilde{\omega}_i f_i = \tilde{\omega}\left(p_i x + q_i y + r_i\right), \quad i = 1, \ldots, 4 \quad (21)$$

The total of the weighted values acquired in the fourth layer is used by the fifth layer to construct the system output as a numerical variable equivalent to the nonfuzzy component in the fuzzy systems, as shown in Equation 22:

$$O_5 = \sum_i \tilde{\omega} f_i \tag{22}$$

The ANFIS model was activated using the fuzzy inference system approach as a five-layered neural network. In a typical ANFIS structure, the first and last layers represent the input variables (spindle speed, depth of cut, and feed rate) and the responses or output variables (MRR and TWR). The model corresponds to first-order Sugeno inference systems, which turn input parameters into membership values via membership functions (MFs) in the second layer using a mechanism known as fuzzification. The model output was then deduced using a set of logical rules in the third layer. In the fourth layer, the inference output was defuzzified to real output values using output membership functions (Zaghloul et al. 2020). The fifth layer used double nodes to display the total of all incoming signals as the overall outputs, which are the material removal and tool wear rates. The ANFIS analysis used the same data sets as the ANN modelling. The Neuro Fuzzy design tool of MATLAB Mathwork GUI was utilized in this study work to develop and evaluate a fuzzy system. Loading data, construction of the Fuzzy Inference System (FIS), and training and testing of the FIS were all possible with the ANFIS editor and the hybrid learning algorithm used for the analysis. Prior to this, a training data set is utilized to search for the constant membership function, and the data set is then error-checked. In general, the ANFIS's performance is measured by the root mean square error between the data and the system output (Sada and Ikpeseni, 2021).

2.3. Statistical Error Indicators Used for Evaluation of the RSM, ANN and ANFIS Models

Different statistical techniques can be used to validate the RSM, ANN, and ANFIS models. The mean absolute bias error (MABE), mean absolute percentage error (MAPE), root mean square error (RMSE), and coefficient of determination (R^2) are the most often used statistical error indicators (Olayode et al., 2023). The average total amount of all the absolute bias errors discovered when comparing the actual and predicted values can be referred to as the mean absolute bias error (MABE). It is represented mathematically as:

$$MABE = \frac{1}{N}\sum_{i=1}^{N}|(V_{i,p} - V_{i,e})| \tag{23}$$

The mean absolute percentage difference (MAPE) between expected and actual responses can be calculated. The mathematical formula for this is:

$$MAPE = \frac{1}{N}\sum_{i=1}^{N}\left|\left(\frac{V_{i,p} - V_{i,e}}{V_{i,e}}\right)\right| \times 100\% \tag{24}$$

The RMSE is determined by knowing the model's accuracy, which is established by comparing the projected and experimental responses, which is necessary to calculate the RMSE. The value is never negative and is always positive. It is denoted mathematically as:

$$RMSE = \sqrt{\frac{1}{N}\sum_{i=1}^{N}(V_{i,p} - V_{i,e})^2} \tag{25}$$

The R^2, also known as the coefficient of determination, signifies the optimal relationship between both the predicted and actual responses. This is mathematically represented as:

$$R^2 = 1 - \frac{\frac{1}{N}\sum_{i=1}^{N}(V_{i,p} - V_{i,e})^2}{\frac{1}{N}\sum_{i=1}^{x}(V_{i,p} - V_{i,avg})^2} \tag{26}$$

where $V_{i,p}$ represents the predicted responses and $V_{i,e}$ indicates the actual responses.

3. Results and Discussions

3.1. Response Surface Modelling

3.1.1. Material removal rate (MRR)

Model fits for the milling process using linear, two (2) Factor interactions (2FI), quadratic, and cubic models. The coefficient of determination (R^2) and standard deviation were the most important metrics for rating the generated models. Because their R^2 values were not close to unity, the linear and 2FI models were not recommended. The cubic model was not proposed since the CCD lacked sufficient runs to justify it (Oguanobi et al. 2019). The quadratic model was suggested since its R^2 value was 0.9996 and its standard deviation was 11.01. This result suggested that the quadratic model can explain 99.96% of the variations in MRR with process variables. The strong R^2 value suggested that the derived models could provide a persuasively good approximation of the response within the examined range.

From this study, if the regression coefficient (R^2) of the modelling process is low, that is, less than 70%, then the mathematical model is not good (Mazaheri et al., 2017). The value of adjusted R^2 was 0.9992, which indicated a good degree of correlation between the experimental and predicted values. The predicted R^2 was 0.9951. These values were within 0.2 of each other, showing that there is no problem with either the data or the model (Taran and

Aghaie, 2015). Furthermore, the predicted R^2 and adjusted R^2 values showed acceptable significance; hence, the quadratic model suggested was adequate.

ANOVA was utilized to analyse the relevance of the model and process parameters, as well as to find the relevant factors in a quadratic model. The F test and p value were used to evaluate the significance of each coefficient. If the p value decreases and the absolute F value increases, then the associated variables become more significant (Amani-Ghadim et al. 2013). The proposed quadratic model was significant since its p value was less than 0.0001 and its F value was 2612.72, indicating appropriate quadratic model fitting. There is only a 0.01% chance that an F value this large could occur due to noise. A 95% confidence interval was employed, which indicates that "Prob > P" values less than 0.05 showed that such model terms are significant. Because the P value was less than 0.05, all the individual and interactions of the process parameters were significant in this scenario. Model reduction, according to Gholamhossein et al. (2016), may enhance the model if there are numerous insignificant model terms.

A standard deviation that is stated as a percentage of the mean is called the coefficient of variation (CV). The lower the CV is, the smaller the residuals are relative to the expected values (Körbahti and Tanyolaç, 2008); the experiment performed in this study has a CV value of 1.25%, indicating great dependability and good accuracy (Gholamhossein et al. 2016). The CV was calculated as the standard deviation divided by the mean of the output variable. A model is considered reproducible if the CV is less than 10%, according to Chen et al. (2011).

The range of predicted values at the design points is compared to the average prediction error to determine adequate precision. An adequate precision ratio (APR) larger than four (4) shows that the model is effective (Noordin et al. 2004); an APR of 187.65 was obtained, which was much higher than the necessary minimum, which suggests good model performance (Okpe et al. 2018; Oguanobi et al. 2019). This was consistent with the findings of Kiomars et al. (2015). The derived quadratic model was Equation 27. The equation was used to model the MRR when milling API 5ST TS-90 alloy using the depth of cut, spindle speed, and feed rate as process parameters.

$$MRR = 925.88 + 92.31A + 171.79B + 466.67C + 44.87AB + 32.05AC - 70.51BC + 223.77A^2 - 96.74B^2 - 212.12C^2 \quad (27)$$

The model equation could be used to make predictions about the response (MRR) for given levels of factors. A positive sign in front of these factors indicates that a rise in such a factor favors the material removal rate (MRR), so it is synergistic, while a negative sign reflects a decrease in such factors, which shows an antagonistic effect. The coefficients associated with a single component A (spindle speed), B (feed rate), and C (depth of cut) indicate the influence of that factor on MRR. The coefficients with two factors (combinations of these elements) and others with second-order terms demonstrate the interaction between the two factors and the quadratic impact. All the model individual and interacting variables were significant in the ANOVA discussion. As a result, no model reduction is needed.

- ***RSM Diagnostic plots for MRR***

In figure 2, graphical estimations were employed in addition to the correlation coefficients to depict the features of the residual (the difference between the experimental and projected values), which is needed for determining the model's fitness and acceptability in modelling the process. Figure 2 depicts the normal probability plot. It was utilized to identify meaningful deviations from normalcy in the model. A normal probability plot plots the sorted data against the values selected. A straight line would be formed by the points on the normal probability plot if the residuals were normal (Lee and Gilmore, 2005). If the data are roughly normally distributed, this plot is required to make the final image seem near a straight line. Departures from a straight line indicate deviations from normalcy (Lee and Gilmore, 2005). The data in the plots were found to be tightly distributed inside the straight line of the plot. This revealed that the model could predict the material removal rate (MRR) within the parameters investigated. The anticipated plot versus actual experimental MRR in Figure 3 shows the quadratic model's suitability in describing the milling process (Iheanacho et al., 2019).

In terms of coded terms, the perturbation graph depicts the departure from the reference point. A deviation's reference point is the mean. As shown in Figure 4, the reference point is 900 mm3/min of MRR. The depth of cut (C) has the greatest deviation, ranging from 200 mm3/min to 1100 mm3/min MRR, with coded values ranging from -1 to +1. Spindle speed (A) had the least amount of deviation, ranging from 1080 to 1300 MRR.

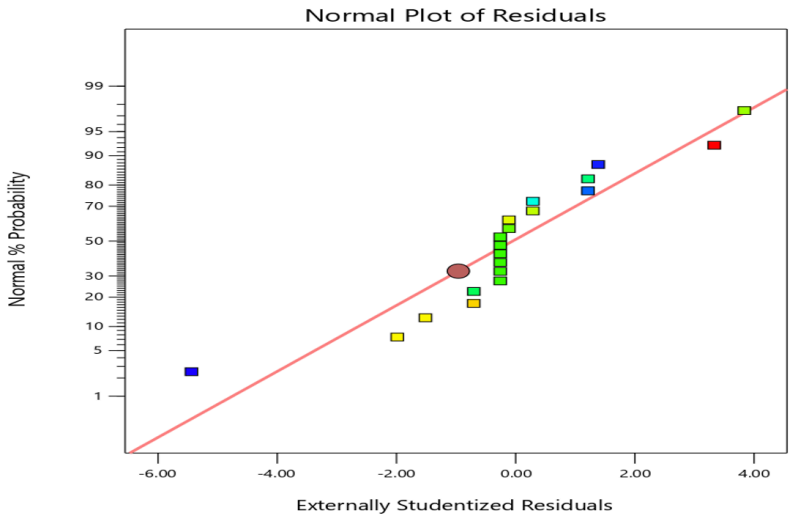

Figure 2. Normal plot of residuals for MRR

doi.org/10.32388/GEGPL7.2

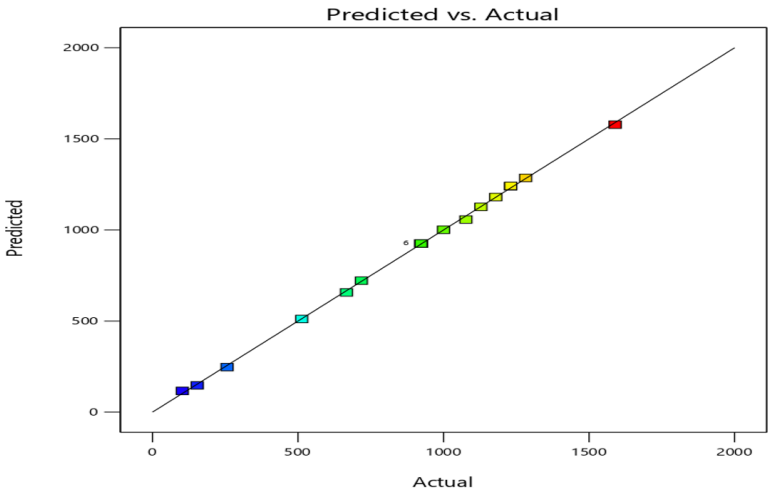

Figure 3. Predicted vs actual plot of residuals for MRR

doi.org/10.32388/GEGPL7.2

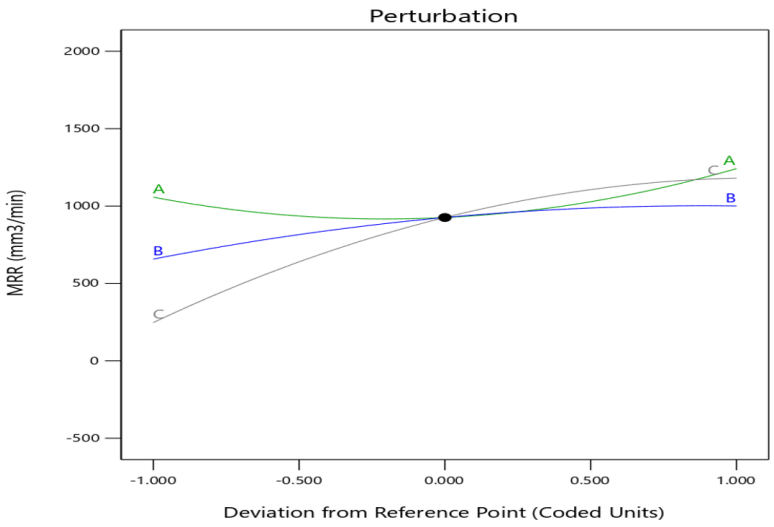

Figure 4. Perturbation plot for MRR

- ***RSM three-dimensional (3D) surface plots and sensitivity analysis for MRR***

The quadratic model's three-dimensional (3-D) surface plots were used to estimate the material removal rate (MRR) and depict the link between the interaction of the experimental variables and the response. The 3-D response surface plots were graphical representations of any two variables' interaction effects, shown as a function of two factors while holding all other factors constant at their null values. Graphical representations such as three-dimensional (3-D) and contour surface plots may be used to explore the interaction impacts of the combination of input factors such as spindle speed, feed rate and depth of cut and response (MRR) (Okpe et al., 2018; Iheanacho et al., 2019).

The elliptical nature of 3-D response surface plots illustrates the synergistic interaction between the two independent variables plotted together and indicates a good interaction of the two variables, whereas the circular shape of the 3D plots indicates no interaction between the variables (Onu et al., 2021). As a result, the elliptical form of the 3D graphs in Figures 5 to 7 reflected all the variables' reciprocal connections. Every two variables had a relatively significant interaction, and the surface restricted in the smallest ellipse in the contour diagrams represented the greatest expected yield.

doi.org/10.32388/GEGPL7.2

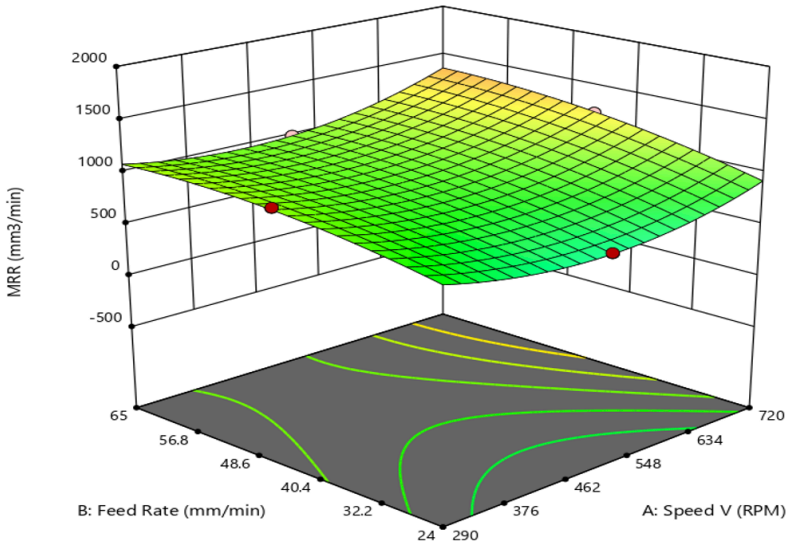

Figure 5. 3D surface plot of feed rate and spindle speed

doi.org/10.32388/GEGPL7.2

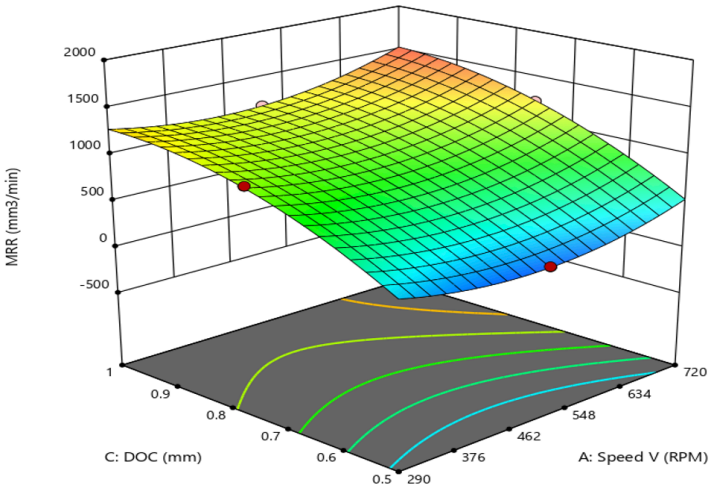

Figure 6. 3D surface plot of the depth of cut and spindle speed

doi.org/10.32388/GEGPL7.2

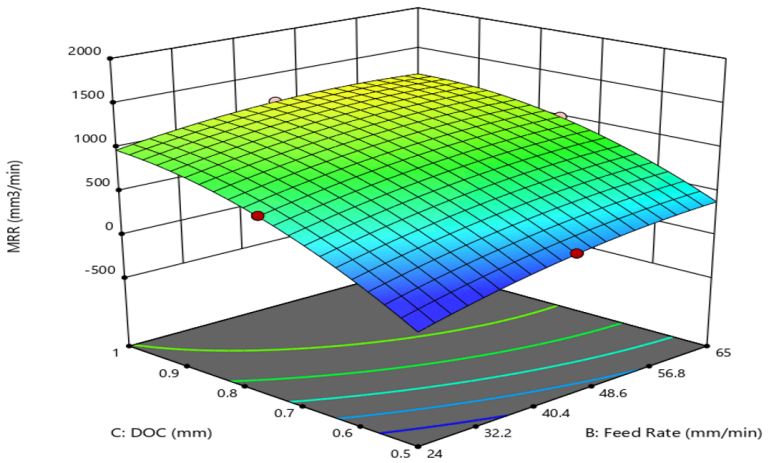

Figure 7. 3D surface plot of the depth of cut and feed rate.

Sensitivity analysis was used to show the influence of each process parameter on the material removal rate in the milling process, as presented in Figure 8. The sensitivity analysis indicated that the depth of cut had the highest influence on the material removal rate, while the spindle speed was the least dominant factor among the factors considered in the milling process. The order of significance of the process parameters on the milling process is as follows: depth of cut > feed rate > spindle speed.

doi.org/10.32388/GEGPL7.2

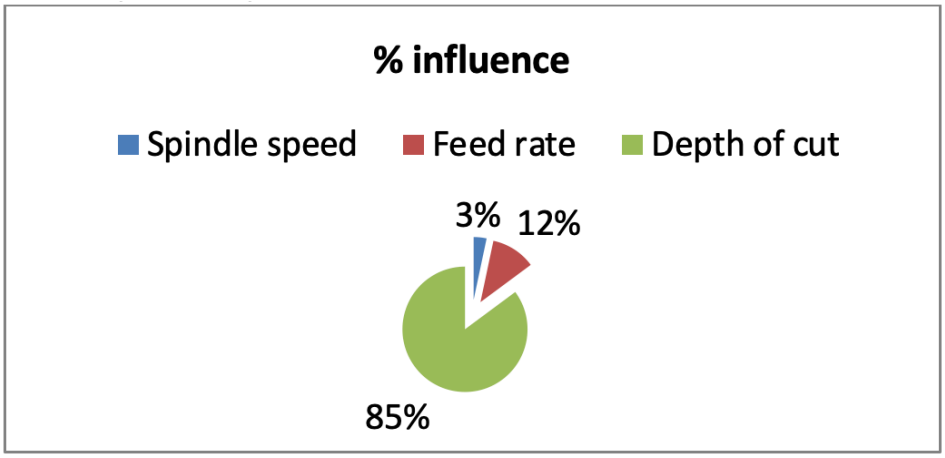

Figure 8. Influence of process parameters in milling API 5ST TS-90 Alloy

3.1.2. Tool Wear Rate (TWR)

Model fits for the milling process using linear, two (2) Factor interactions (2FI), quadratic, and cubic models. The coefficient of determination (R^2) and standard deviation were the most important metrics for rating the generated models. Because the R^2 values of other models were not close to unity apart from the 2FI, the two-factor interaction (2FI) model was recommended since its R^2 value was 0.9904 and its standard deviation was 0.0544. The cubic model was not proposed since the CCD lacked sufficient runs to justify it (Oguanobi et al. 2019). This result suggested that the 2FI model can explain 99.04% of the variations in TWR with process variables. The strong R^2 value suggested that the derived models could provide a good approximation of the response within the examined range. From this study, if the regression coefficient (R^2) of the modelling process is low, that is, less than 70%, then the mathematical model is not good (Mazaheri et al., 2017).

The value of adjusted R^2 was 0.9859, which indicated a good degree of correlation between the experimental and predicted values. The predicted R^2 was 0.9629. These values were within 0.2 of one another, demonstrating that neither the data nor the model were flawed (Taran and Aghaie, 2015). Furthermore, the predicted R^2 and adjusted R^2 values showed acceptable significance; hence, the 2FI model suggested was adequate.

ANOVA was utilized to analyse the relevance of the model and process parameters, as well as to find the relevant factors in a 2FI model. The F test and p value were used to evaluate the significance of each coefficient. If the p value decreases and the absolute F value increases, then the associated variables become more significant (Amani-Ghadim et al. 2013).

The proposed 2FI model was significant since its p value was less than 0.0001 and its F value was 222.74, indicating appropriate model fitting. There is only a 0.01% chance that an F value this large could occur due to noise. A 95% confidence interval was employed, which indicates that "Prob > P" values less than 0.05 showed that such model terms are significant. Because the P value was less than 0.05, some of the individual and interactions of the process parameters were significant in this scenario. Model reduction, according to Gholamhossein et al. (2016), may enhance the model if there are numerous insignificant model terms.

An APR of 55.84 was obtained, which was much higher than the necessary minimum, which suggests good model performance (Okpe et al. 2018; Oguanobi et al. 2019). This was consistent with the findings of Kiomars et al. (2015). The experiment performed in this study has a CV value of 5.54%, indicating great dependability and good accuracy (Gholamhossein et al. 2016). Multiple regression analysis was performed to correlate the response (tool wear rate - TWR) with the three factors evaluated using a second-order polynomial equation (depth of cut, spindle speed, and feed rate). The derived 2FI model is shown in Equation 28. The equation was used to model the TWR when milling API 5ST TS-90 alloy using the depth of cut, spindle speed, and feed rate as process parameters.

$$TWR = 0.9810 + 0.05A + 0.452B + 0.396C - 0.0175AB + 0.0025AC + 0.1975BC \quad (28)$$

The coefficients associated with a single component (A (spindle speed), B (feed rate), and C (depth of cut) indicate the influence of that factor on TWR. The coefficients with two factors (combinations of these elements) represent the

doi.org/10.32388/GEGPL7.2

interaction between the two factors. All the model individual and interacting variables were significant apart from AB and AC in the ANOVA discussion. As a result, model reduction was needed; the insignificant terms were AB and AC since their respective p values were above 0.05. Therefore, eliminating the insignificant terms, the final model equation will be as expressed in Equation 29.

doi.org/10.32388/GEGPL7.2

$$TWR = 0.9810 + 0.05A + 0.452B + 0.396C + 0.1975BC \quad (29)$$

The model equation 29 could be used to predict the response for the given level of factors. It was also effective for determining the relative importance of the factors by comparing their coefficients.

- ***RSM Diagnostic plots for TWR***

Figure 9 depicts the normal probability plot. The straight line of the plot revealed that the model could predict the tool wear rate (TWR) within the parameters investigated. The plot of anticipated versus actual experimental TWR in Figure 10 shows the 2FI model's suitability in describing the milling process (Iheanacho et al., 2019). The perturbation graph is shown in Figure 11, and the reference point is 0.98 mm/min of TWR. The feed rate (B) has the greatest deviation, ranging from 0.5 mm/min to 1.4 mm/min TWR, with coded values ranging from -1 to +1. Spindle speed (A) had the least amount of deviation, ranging from 0.93 to 1.03 TWR.

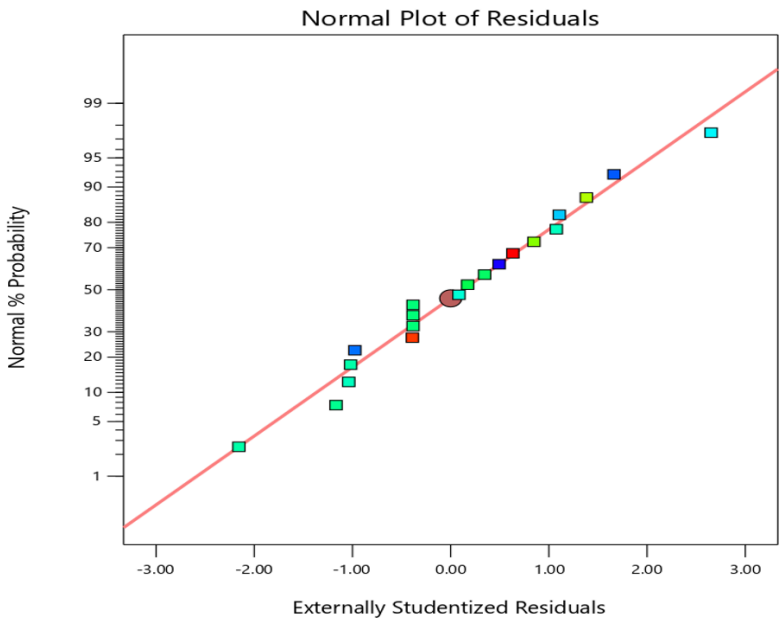

Figure 9. Normal plot of residuals

doi.org/10.32388/GEGPL7.2

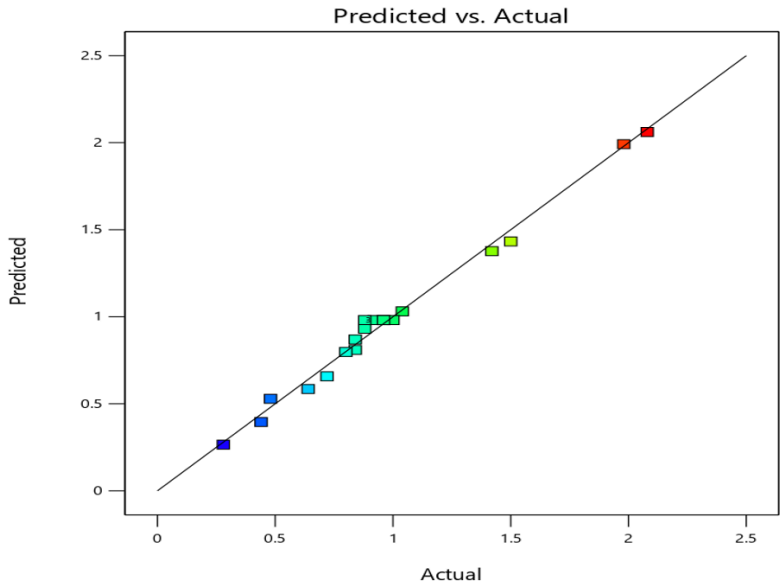

Figure 10. Predicted versus actual plot of residuals

doi.org/10.32388/GEGPL7.2

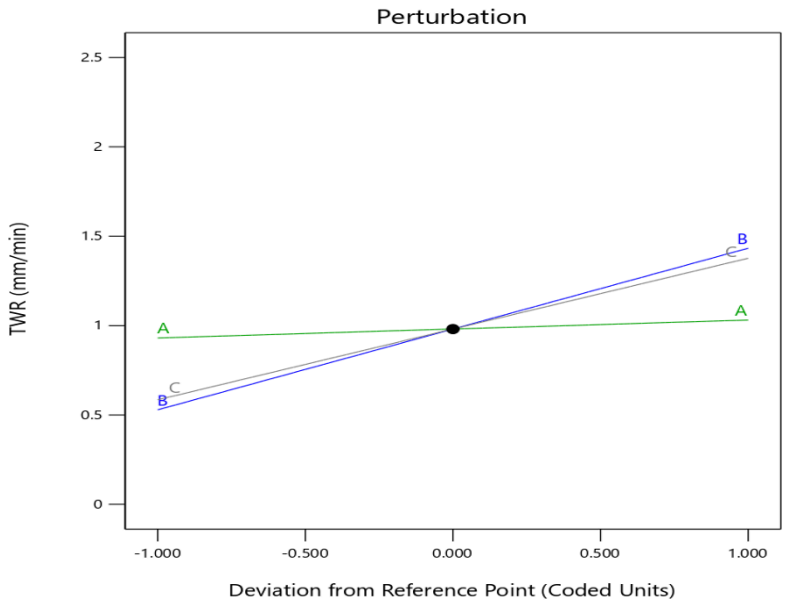

Figure 11. Perturbation plot

- ***RSM three-dimensional (3D) surface plots and sensitivity analysis for TWR***

The 3D graphs in Figures 12 to 14 reflect all the variables' reciprocal connections. B (feed rate) and C (depth of cut) are the two variables that had a relatively significant interaction, and the surface restricted in the smallest ellipse in the contour diagrams represented the greatest expected yield.

doi.org/10.32388/GEGPL7.2

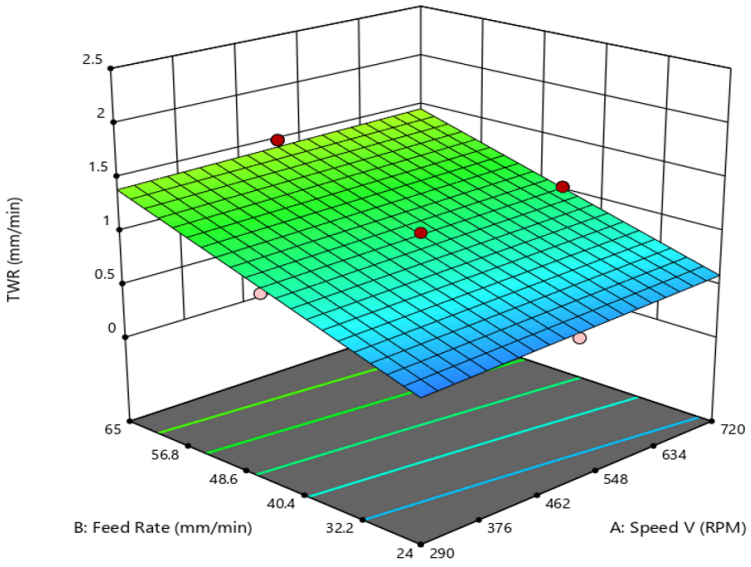

Figure 12. 3D surface plot of feed rate and spindle speed

doi.org/10.32388/GEGPL7.2

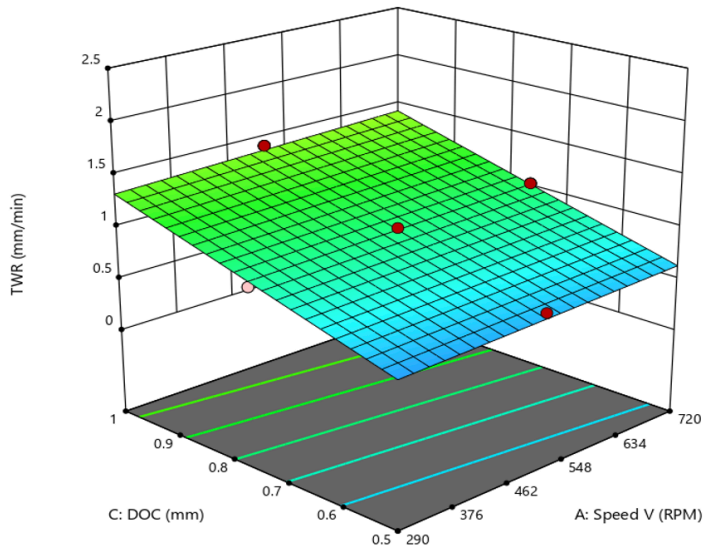

Figure 13. 3D surface plot of the depth of cut and spindle speed

doi.org/10.32388/GEGPL7.2

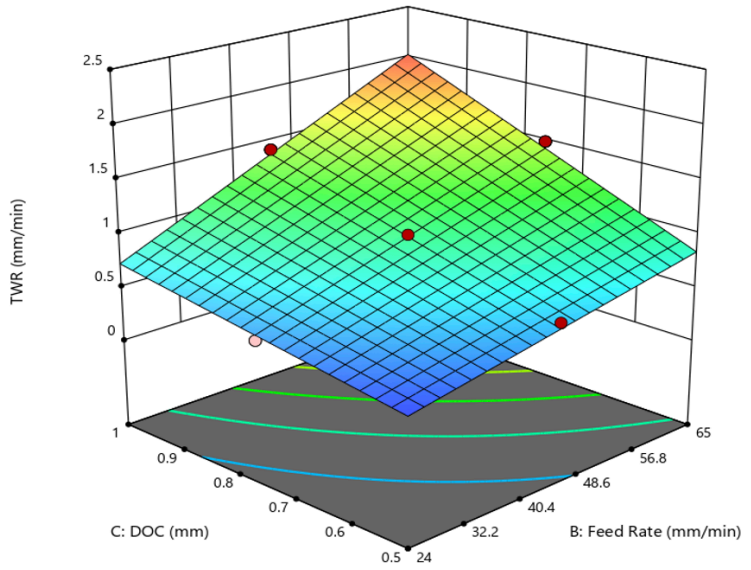

Figure 14. 3D surface plot of the depth of cut and feed rate.

Sensitivity analysis was used to show the influence of each process parameter on the tool wear rate in the milling process, which is presented in Figure 15. The sensitivity analysis indicated that feed rate has the highest influence on the tool wear rate, while spindle speed was the least dominant factor among the factors considered in the milling process. The order of significance of the process parameters on the drying process is as follows: feed rate > depth of cut > spindle speed.

doi.org/10.32388/GEGPL7.2

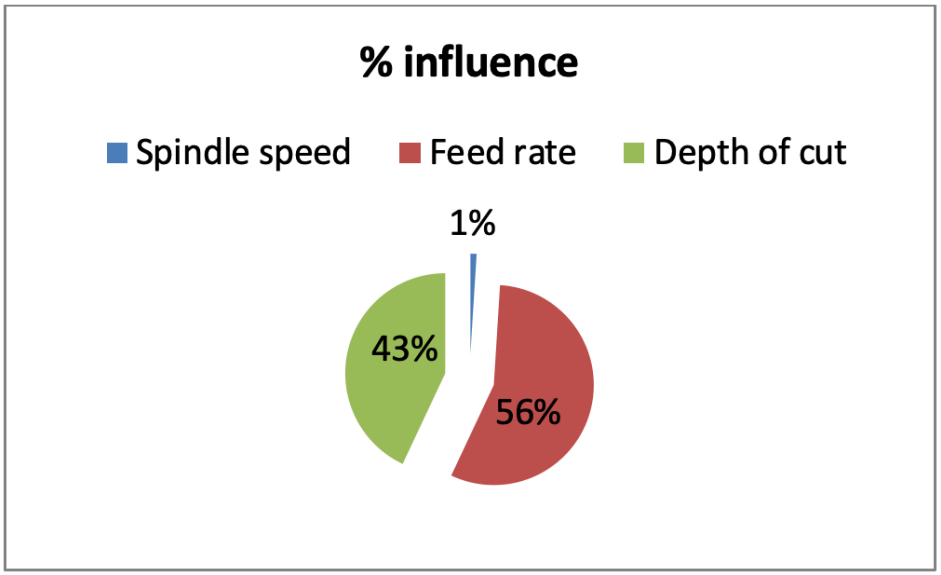

Figure 15. Influence of process parameters on TWR in milling API 5ST TS-90 Alloy

3.2. ANN Modelling for MRR and TWR

ANN modelling was conducted using MATLAB 2022b. Data were divided so that 70% was utilized for training, 15% for validation, and 15% for testing. This translates to 14 training data sets, 3 validation data sets, and 3 testing data sets. More data sets assigned to training prevent overparameterization (Jamil et al. 2018). To find the ideal number of neurons in the hidden layer using the trial-and-error method, the lowest mean squared error (MSE) and highest correlation coefficient were utilized as performance checks. The hidden layer in this scenario has eight ideal neurons. The ANN architecture for the milling process was therefore 3-8-2, which corresponds to 3 neurons in the input layer, 8 neurons in the hidden layer, and 2 neurons in the output layer. Levenberg–Marquardt (LM) back propagation was the algorithm utilized in the ANN modelling. The regression coefficient and the mean square error at the optimum ANN architecture are tabulated in Table 6, and the properties of the ANN modelling are given in Table 7.

doi.org/10.32388/GEGPL7.2

Objective	Number of samples	Mean square error	Regression value
Training	14	1.1429e-04	1
Validation	3	1.1000e-03	1
Testing	3	-	0.99867

Table 6. Regression values and the mean square errors for 8 neurons in the hidden layer

doi.org/10.32388/GEGPL7.2

Algorithm	Back propagation
Error function	Mean square error
Input layer neuron	3
Hidden layer neuron	8
Output layer neuron	2
Training	Levenberg-Maraquardt
Hidden layer	Trainlm
Data division	Dividerand

Table 7. Properties of the ANN model

Figure 16 shows the regression graphs for the training, validation, testing, and entire network process in relation to the targets. The correlation coefficients obtained for the training, validation, testing and overall neural network processes were 1, 1, 0.99867, and 0.99698, respectively. The plot of the validation performance is presented in Figure 17. The performance of the network process for validation was analysed to determine the reliability of the training process. The training network showed a validation performance with a mean square error of 1.0667e-03 at epoch 7.

doi.org/10.32388/GEGPL7.2

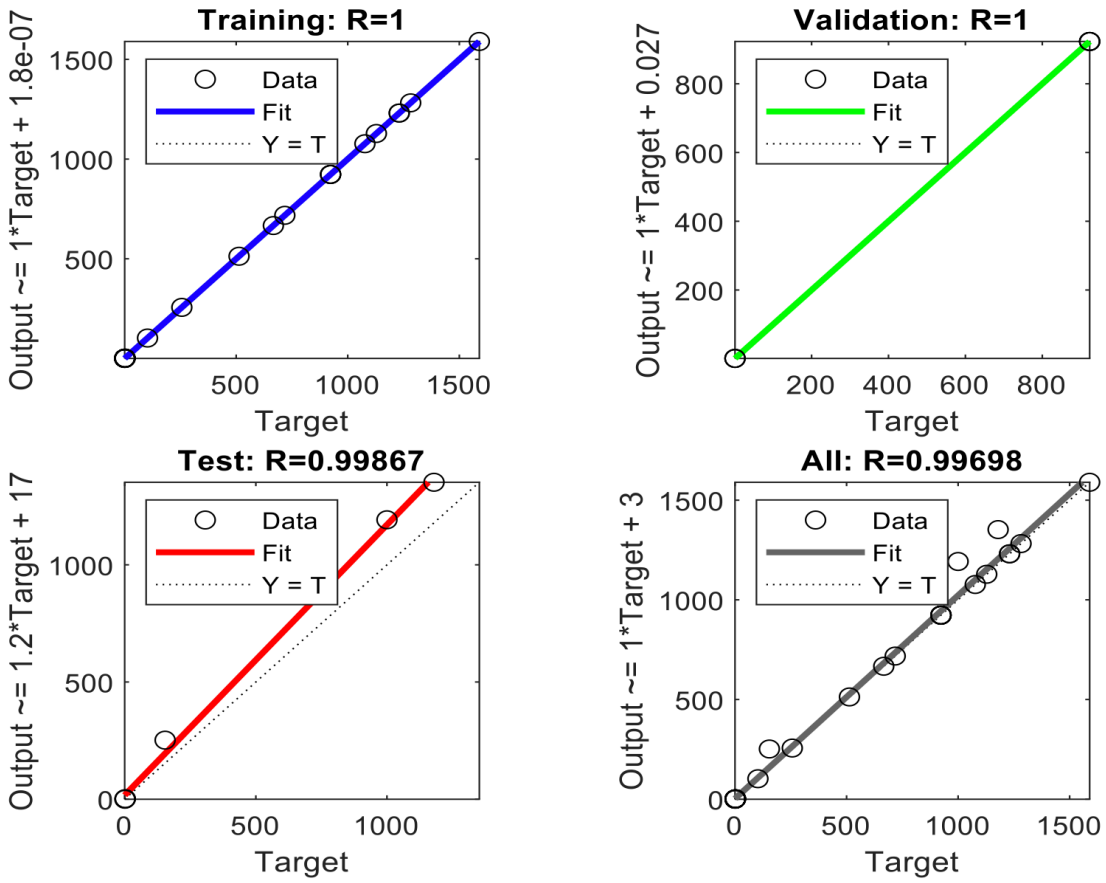

Figure 16. Regression plots for training, validation, test, and all (overall) for the ANN model.

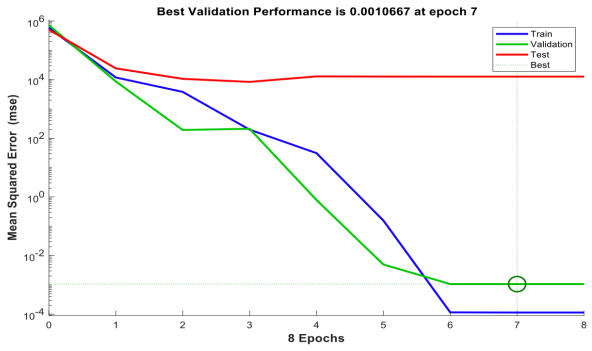

Figure 17. ANN validation performance of the milling process

the three input factors (spindle speed, depth of cut, and feed rate), as well as 20 samples of the single output variable (material removal rate) and was also replicated for TWR. The least squares and gradient methods were used to create the ANFIS model's structural framework. The *Gaussmf* membership function was used in the grid partition check. The hybrid train FIS optimization approach was used to train the generated data with the help of the *Gaussmf* membership function (Shukry et al., 2018).

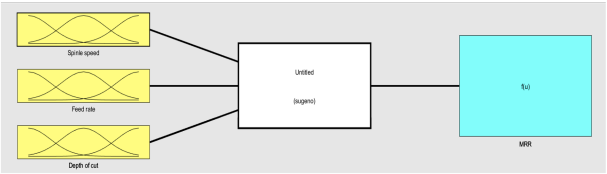

Figure 18. High-level fuzzy architecture for the MRR model

3.3. ANFIS Modelling for MRR and TWR

The experimental data were entered into a MATLAB m-file as a 20x4 matrix, which represented 20 samples of each of

doi.org/10.32388/GEGPL7.2

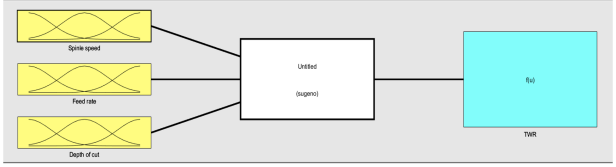

Figure 19. High-level fuzzy architecture for the TWR model

Figures 20 and 21 show that the fuzzy inference system (FIS) output significantly tracked the training data for the milling process.

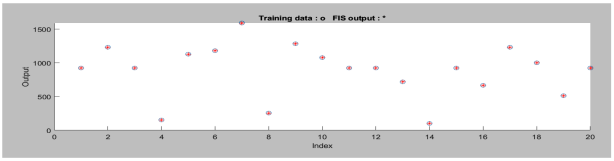

Figure 20. ANFIS training data against FIS output data for MRR

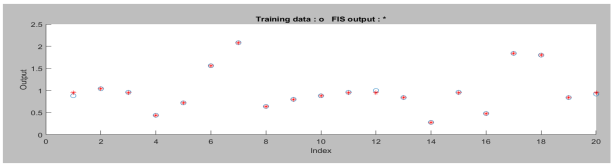

Figure 21. ANFIS training data against FIS output data for TWR

The ANFIS data were trained at an error tolerance of 0.0001 and 100 epoch iterations. The training produced an error magnitude of 0.001222, which stabilized at 100 epochs of training for MRR, and an error magnitude of 0.020656, which stabilized at 100 epochs of training for TWR. The low mean square error value obtained showed that there was no overfitting in the training process and that the ANFIS model can satisfactorily predict the MRR and TWR in milling API 5ST TS-90 alloy.

3.4. Model Prediction and Comparison

The MRR and TWR predictive efficiency of the trained RSM, ANN, and ANFIS models' predictions were compared. The comparisons were based on the MRR and TWR predictions of the models at the experimental conditions for the twenty data sets. The experimental or observed values and predicted values together with the calculated residual values are highlighted in Tables 8 and 9 for the material removal rate (MRR) and tool wear rate (TWR), respectively. The residual was calculated as the difference between each experimental value and its corresponding predicted value.

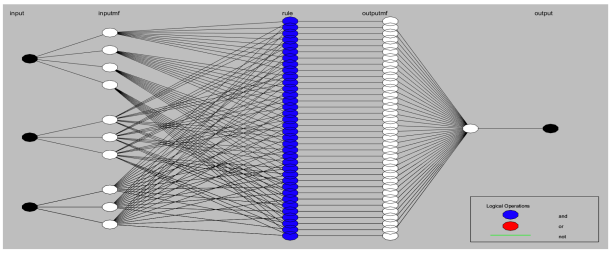

Figure 22. ANFIS model structure for MRR and TWR

doi.org/10.32388/GEGPL7.2

S/N	Experimental MRR(mm^3/min)	RSM		ANN		ANFIS	
		Predicted MRR	Residual	Predicted MRR	Residual	Predicted MRR	Residual
1	923.08	925.88	-2.8	924	-0.92	923	0.08
2	1230.77	1241.96	-11.19	1226	4.77	1230	0.77
3	923.08	925.88	-2.8	924	-0.92	923	0.08
4	153.85	147.21	6.64	154.4	-0.55	153	0.85
5	1128.21	1126.29	1.92	1128	0.21	1128	0.21
6	1179.49	1180.42	-0.93	1233	-53.51	1180	-0.51
7	1589.74	1577.97	11.77	1586	3.74	1590	-0.26
8	256.41	247.09	9.32	253	3.41	256	0.41
9	1282.05	1285.66	-3.61	1256	26.05	1280	2.05
10	1076.92	1057.34	19.58	1228	-151.08	1080	-3.08
11	923.08	925.88	-2.8	924	-0.92	923	0.08
12	923.08	925.88	-2.8	924	-0.92	923	0.08
13	717.95	721.56	-3.61	710	7.95	718	-0.05
14	102.56	116.43	-13.87	145	-42.44	103	-0.44
15	923.08	925.88	-2.8	924	-0.92	923	0.08
16	666.67	657.35	9.32	605.5	61.17	667	-0.33
17	1230.77	1239.51	-8.74	1249	-18.23	1230	0.77
18	1000	1000.93	-0.93	1102	-102	1000	0
19	512.82	511.3	1.52	495.6	17.22	513	-0.18
20	923.08	925.88	-2.8	924	-0.92	923	0.08

Table 8. RSM, ANN, and ANFIS comparative analysis for MRR in milling API 5ST TS-90 alloy:

doi.org/10.32388/GEGPL7.2

S/N	Experimental TWR (mm/min)	RSM	ANN	ANFIS			
		Predicted TWR	Residual	Predicted TWR	Residual	Predicted TWR	Residual
1	0.88	0.981	-0.101	0.9121	-0.0321	0.947	-0.067
2	1.04	1.03	0.01	0.6709	0.3691	1.04	0
3	0.96	0.981	-0.021	0.9121	0.0479	0.947	0.013
4	0.44	0.3955	0.0445	0.4613	-0.0213	0.44	0
5	0.72	0.6575	0.0625	0.7174	0.0026	0.72	0
6	1.56	1.38	0.18	1.55	0.01	1.56	0
7	2.08	2.06	0.02	1.601	0.479	2.08	0
8	0.64	0.585	0.055	0.634	0.006	0.64	0
9	0.8	0.7975	0.0025	0.8172	-0.0172	0.8	0
10	0.88	0.931	-0.051	0.8567	0.0233	0.88	0
11	0.96	0.981	-0.021	0.9121	0.0479	0.947	0.013
12	1	0.981	0.019	0.9121	0.0879	0.947	0.053
13	0.84	0.8695	-0.0295	0.86	-0.02	0.84	0
14	0.28	0.2655	0.0145	0.504	-0.224	0.28	0
15	0.96	0.981	-0.021	0.9121	0.0479	0.947	0.013
16	0.48	0.529	-0.049	0.4756	0.0044	0.48	0
17	1.84	1.99	-0.15	2.053	-0.213	1.84	0
18	1.8	1.43	0.37	1.775	0.025	1.8	0
19	0.84	0.8095	0.0305	0.785	0.055	0.84	0
20	0.92	0.981	-0.061	0.9121	0.0079	0.947	-0.027

Table 9. RSM, ANN, and ANFIS comparative analysis for TWR in milling API 5ST TS-90 alloy

The plots of experimental MRR against predicted MRRs by the ANN, ANFIS, and RSM models are presented in Figures 23 to 25 for MRR and Figures 26 to 28 for TWR. The high correlation of the figures supported the assertion that the three models have excellent correlation and adequate predictive ability in predicting MRR and TWR during the milling process. The coefficients of determination obtained were all greater than 0.85, indicating that all three models were relatively adequate in modelling and predicting the MRR and TWR. However, for MRR, ANFIS (R^2 = 1) and RSM (R^2 = 0.9996) were marginally better than ANN (R^2 = 0.9867) in the predicted material removal rate for the milling process. For TWR, ANFIS (R^2 = 0.998) and RSM (R^2 = 0.9488) were slightly better than ANN (R^2 = 0.8929) in the predicted tool wear rate for the milling operation.

doi.org/10.32388/GEGPL7.2

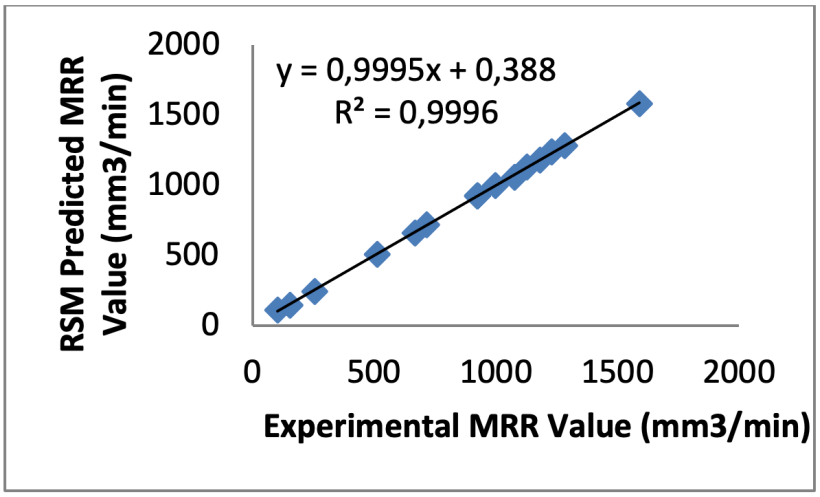

Figure 23. Experimental against RSM-predicted MRR for milling API 5ST TS-90 alloy

doi.org/10.32388/GEGPL7.2

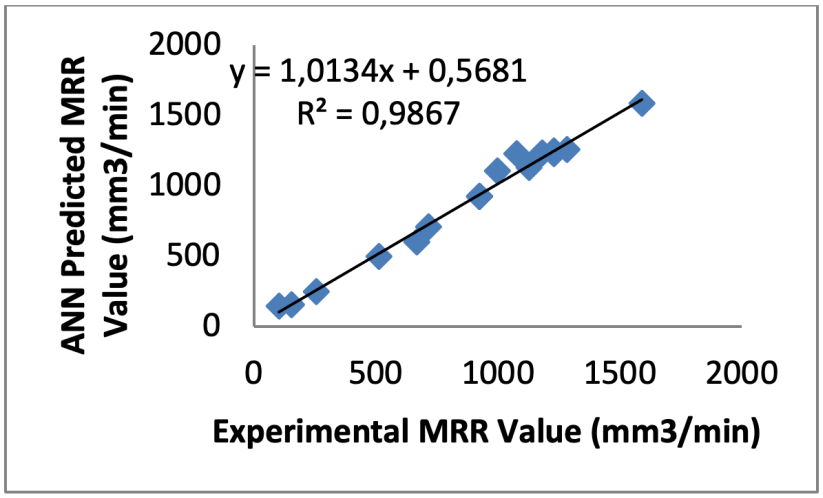

Figure 24. Experimental against ANN-predicted MRR for milling API 5ST TS-90 alloy

doi.org/10.32388/GEGPL7.2

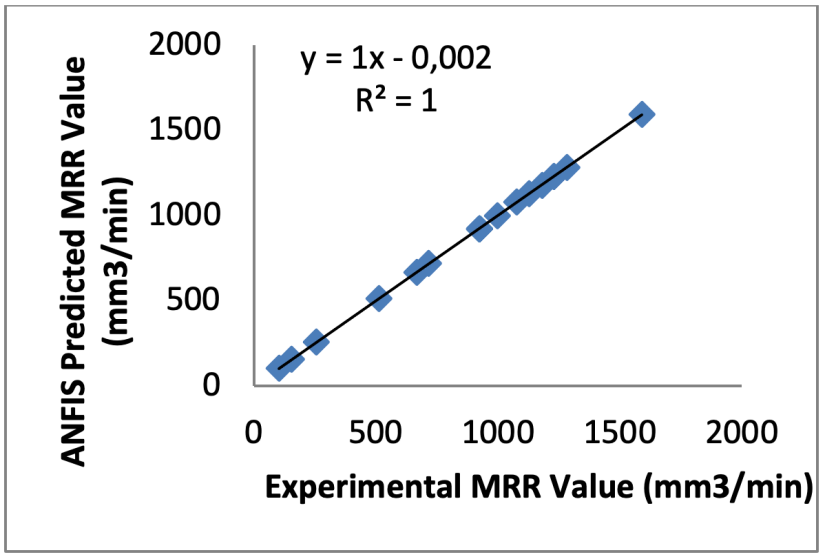

Figure 25. Experimental against ANFIS-predicted MRR for milling API 5ST TS-90 alloy

doi.org/10.32388/GEGPL7.2

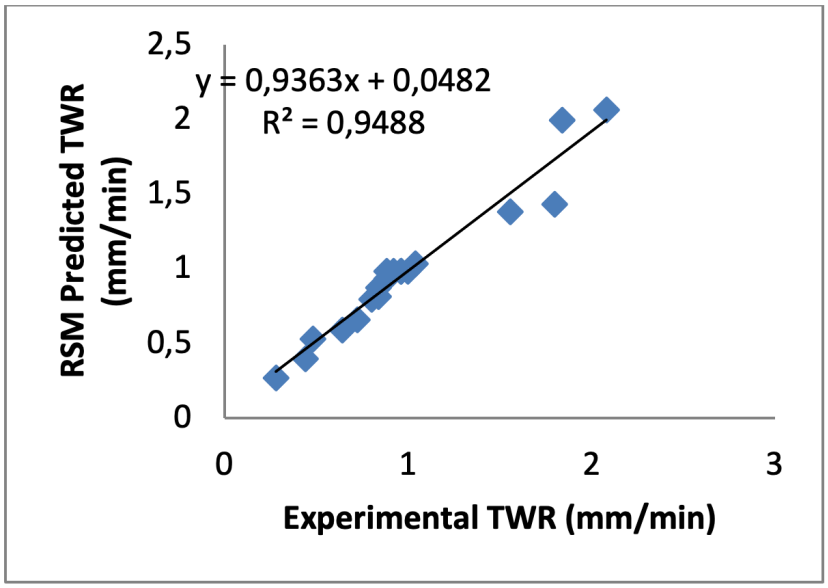

Figure 26. Experimental against RSM predicted TWR for milling API 5ST TS-90 alloy

doi.org/10.32388/GEGPL7.2

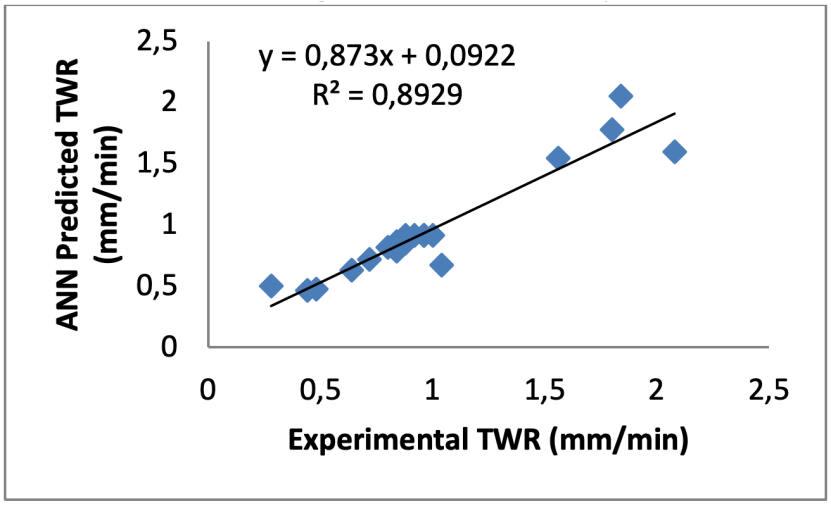

Figure 27. Experimental against ANN predicted TWR for milling API 5ST TS-90 alloy

doi.org/10.32388/GEGPL7.2

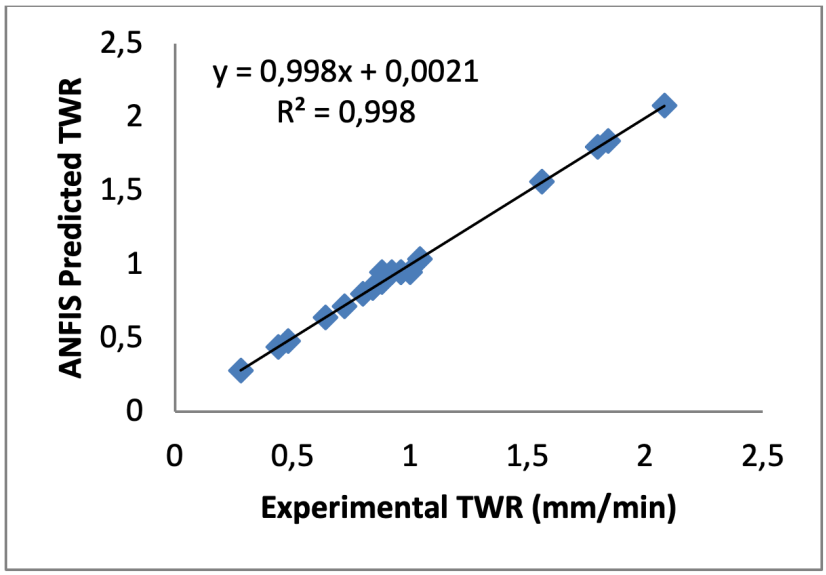

Figure 28. Experimental against ANFIS predicted TWR for milling API 5ST TS-90 alloyThe statistical error indicators used for the evaluation of the ANN, RSM and ANFIS models for MRR and TWR are shown in Table 10.

doi.org/10.32388/GEGPL7.2

Statistical indicators	RSM		ANN		ANFIS	
	MRR	TWR	MRR	TWR	MRR	TWR
MABE	5.9875	0.0657	24.8925	0.0871	0.5195	0.0093
MAPE	1.5147%	6.2383%	4.5113%	10.0586%	0.0967%	0.9956%
RMSE	7.7927	0.1058	46.4004	0.1553	0.9087	0.0207
R^2	0.9996	0.9488	0.9867	0.8929	1.000	0.998

Table 10. Statistical indicators for RSM, ANN, and ANFIS for MRR and TWR

Comparatively, ANFIS (R^2 = 1, MABE=0.5195, MAPE=0.0967%, RMSE=0.9087) and RSM (R^2 = 0.9996, MABE=5.9875, MAPE=1.5147%, RMSE=7.7927) were marginally better than ANN (R^2 = 0.9867, MABE=24.8925, MAPE=4.5113%, RMSE=46.4004) in the predicted material removal rate for the milling process. For the tool wear rate, ANFIS (R^2 = 0.998, MABE=0.0093, MAPE=0.9956%, RMSE=0.0207) and RSM (R^2 = 0.9488, MABE=0.0657, MAPE=6.2383%, RMSE=0.1058) were slightly better than ANN (R^2 = 0.8929, MABE=0.0871, MAPE=10.0586%, RMSE=0.1553) in the predicted tool wear rate for the milling operation. Generally, ANFIS showed a better predictive capability than RSM and ANN for both MRR and TWR.

3.5. Optimization and validation of the milling process

The optimization of the milling process was performed with the aid of the numerical optimization tool of CCD-RSM in Design Expert Software. The MRR was set at a maximum, and the TWR was set at a minimum to achieve optimum milling operation. Increased production at a lower tooling cost was the target of the optimization procedure. Forty-five (45) different solutions of optimization desirability were proposed by the central composite design for the milling operation. The desirability values range from 0 to unity based on how close the response is to the objective. The closer the desirability is to one, the better the accuracy. For the milling process, condition 1 of the optimization condition suggested by the CCD-RSM was selected with predicted optimum MRRs of 1272.163 mm3/min and 0.781 mm/min for TWR. The optimum milling process was validated under the suggested experimental conditions by carrying out a milling experiment under those conditions. The test-retest method was used, and the mean MRR and TWR were selected. The results tabulated in Table 11 show a close correlation between the predicted and validated optimum MRR and TWR.

doi.org/10.32388/GEGPL7.2

Responses	Predicted optimum conditions			Predicted optimum	Validated optimum
	Spindle speed	Feed rate	Depth of cut		
MRR	720.00	24.00	0.979	1272.163	1270.05
TWR	720.00	24.00	0.979	0.781	0.77

Table 11. Optimum MRR, TWR and validation

4. Conclusion

From this study, the RSM, ANN, and ANFIS models were effectively used in predicting and modelling the milling process with a coefficient of determination above 0.85. Comparatively, the ANFIS model gave marginally better MRR and TWR predictions than ANN and RSM, while RSM gave a better prediction than ANN. The optimum process milling parameters (i.e., feed rate, spindle speed and depth of cut) for a better material removal rate (MRR) and tool wear rate (TWR) were obtained as a 720 rpm spindle speed, 24 mm/min feed rate and 0.979 mm depth of cut to achieve the best output of 1272.163 mm3/min MRR and reduced tool wear rate of 0.781 mm/min. The optimum milling process was validated under the suggested experimental conditions by carrying out a milling experiment under those conditions, and the results showed a close correlation between the predicted and validated optimum values. The optimum milling parameters obtained from this study would give machinists and production engineers the opportunity to have an improved production process and reduced tooling cost often associated with tool wear.

References

- Abbas, S.T., (2013). Modelling and optimization of adsorption of heavy metal ions onto local activated carbon. Aquatic Science Technology, 1 (2), 108–134.
- Amani-Ghadim, A.R., Aber, S., Olad, A. & Ashassi-Sorkhabi, H. (2013). Optimization of electrocoagulation process for removal of an azo dye using response surface methodology and investigation on the occurrence of destructive side reactions. Chemical Engineering and Processing, 64, 68-78
- Arulkumar, M., Sathishkumar, P. & Palvannan, T. (2011). Optimization of orange G dye adsorption by activated carbon of thespesia populnea pods using response surface methodology. Journal of Hazard Materials, 186 (1), 827–834. https://doi.org/10.1016/j.jhazmat.2010.11.067
- Asadi, R., Yeganefar, A. & Niknam, S.A. (2019). Optimization and prediction of surface quality and cutting forces in the milling of aluminum alloys using ANFIS and interval type 2 neuro fuzzy networks coupled with population-based meta-heuristic learning methods. International Journal of Advanced Manufacturing Technology, 105, 2271–2287. https://doi.org/10.1007/s00170-019-04309-6
- Bagga, P.J., Makhesana, M.A., Patel, H.D. & Patel, K.M. (2021). Indirect method of tool wear measurement and prediction using ANN network in machining process. Materials Today: Proceedings, 44(1), 1549-1554. https://doi.org/10.1016/j.matpr.2020.11.770.
- Banza, M., Seodigeng, T. & Rutto, H. (2023). Comparison Study of ANFIS, ANN, and RSM and Mechanistic Modelling for Chromium(VI) Removal Using Modified Cellulose Nanocrystals–Sodium Alginate (CNC–Alg). Arabian Journal for Science and Engineering. https://doi.org/10.1007/s13369-023-07968-6
- Bouzid, L., Yallese, M.A., Belhadi, S., & Haddad, A. (2020). Modelling and optimization of machining parameters during hardened steel AISID3 turning using RSM, ANN and DFA techniques: comparative study. Journal of Mechanical Engineering and Sciences, 14(2), 6835-8380. https://doi.org/10.15282/jmes.14.2.2020.23.0535
- Chabbi, A., Yallese, M., Nouioua, M., Meddour, I., Mabrouki, T., & Girardin, F. (2017). Modelling and optimization of turning process parameters during the cutting of polymer (POM C) based on RSM, ANN, and DF methods. The International Journal of Advanced Manufacturing Technology, 91(5), 2267-2290. https://doi.org/10.1007/s00170-016-9858-8
- Chen, G., Chen, J., Srinivasakannan, C. & Peng, J., (2011). Application of response surface methodology for optimization of the synthesis of synthetic rutile from titania slag. Applied Surface Science, 258 (7), 3068–3073. https://doi.org/10.1016/j.apsusc.2011.11.039
- Coppini, N.L. & dos Santos, I.A. (2015). Increasing Production and Minimizing Costs During Machining by Control of Tool's Wears and or Damages. Enhancing

Synergies in a Collaborative Environment. 235-245. https://doi.org/10.1007/978-3-319-14078-0_27
- Daniel, J. S. C., Yi, J. C., Senthil, K. A., Sara, K. Y. & Jun, W. L. (2023). Optimization and performance evaluation of response surface methodology (RSM), artificial neural network (ANN) and adaptive neuro-fuzzy inference system (ANFIS) in the prediction of biogas production from palm oil mill effluent (POME). Energy, 266, 126449. https://doi.org/10.1016/j.energy.2022.126449.
- Datta, S., Nandi, G., Bandyopadhyay, A & Pal, P.K. (2010). Optimization of end milling process parameters using PCA-based Taguchi Method. International Journal of Engineering, Science and Technology, 2(1), 92-102
- Gholamhossein, S., Seyed, A.S., Nedasadat, S.A. (2016). Evaluation of the response surface and hybrid artificial neural network-genetic algorithm methodologies to determine extraction yield of ferulago angulate through supercritical fluid. Journal of the Taiwan Institute of Chemical Engineers, 60, 165-173.
- Haykin, S. (2008). Neural Networks and Learning Machines, third ed., Pearson Prentice Hall.
- Himanshu, P., Sharma, S.K., Aakash, A. k. & Avinash, K. (2019). Study of MRR and TWR in Electric Discharge Machining of AISI D2 Tool Steel. Advances in Industrial and Production Engineering. Springer. https://doi.org/10.1007/978-981-13-6412-9_8
- Hsu, Q.C., & Nguyen, H.T. (2017). Study on cutting forces and material removal rate in hard milling of SKD 61 alloy steel, Journal of the Chinese society of mechanical engineers, 38(1), 41-51
- Iheanacho, C.O., Nwabanne, J.T., Onu, C.E. (2019). Optimum process parameters for activated carbon production from rice husk for phenol adsorption. Current Journal of Applied Science and Technology, 36(6), 1-11. https://doi.org/10.9734/CJAST/2019/v36i630264
- Kiomars, S., Meghdad, P., Mitra, M., Amir, M. M., Ali, A.L.Z. and Sethupathi, S. (2015). Process modelling and optimization of biological removal of carbon, nitrogen and phosphorus from hospital wastewater in a continuous feeding & intermittent discharge (CFID) bioreactor. Korean Journal of Chemical Engineering, 32(7), 1340-1353. https://doi.org/10.1007/s11814-014-0365-z
- Körbahti, B.K. & Tanyolaç, A. (2008). Electrochemical treatment of simulated textile wastewater with industrial components and Levafix Blue CA reactive dye: Optimization through response surface methodology. Journal of Hazard Materials, 151, 422–431.
- Kumar, U., Singh, A. & Kumar, R. (2016) Optimization of Machining Parameters for Tool Wear Rate and Material Removal Rate in CNC turning by Grey Relational Analysis. International Journal of Applied Engineering Resources, 11(4), 973–4562
- Kundrak, J., Molnar, V. & Deszpoth, I. (2018). Analysis of Machining Time and Material Removal Performance as Factors Influencing Efficiency and Profitability. Vehicle and Automotive Engineering 2, 268-279. https://doi.org/10.1007/978-3-319-75677-6_22
- Lee, K.M. & Gilmore, D.F. (2005) Formulation and process modelling of biopolymer (polyhydroxyalkanoates: PHAs) production from industrial wastes by novel crossed experimental design. Process Biochemistry, 40, 229–246.
- Liu, C., Ren, J. & Zhang, Y. (2023). The Effect of Tool Structure and Milling Parameters on the Milling Quality of CFRP Based on 3D Surface Roughness. Internationlal Journal of Precision Engineering and Manufacturing, 24, 931–944. https://doi.org/10.1007/s12541-023-00799-3
- Lotfan, S.R., Ghiasi, A. & Fallah, M. (2016). ANN-based modelling and reducing dual-fuel engine's challenging emissions by multiobjective evolutionary algorithm NSGA-II. Journal of Applied Energy, 175, 91–99.
- Long, W., Xingchen, Y. & Liang, G. (2020) A new automatic machine learning based hyper parameter optimization for workpiece quality prediction. Measurement Controls, 53 (7- 8), 1088–1098.
- Mathur, N., Glesk, I. & Buis, A. (2016). Comparison of adaptive neuro-fuzzy inference system (ANFIS) and Gaussian processes for machine learning (GPML) algorithms for the prediction of skin temperature in lower limb prostheses, *Medical Engineering Physics*, 38, 1083–1089
- Mazaheri, H., Ghaedi, M., Ahmadi, A.M.H., Asfaram, A. (2017). Application of Machine/Statistical Learning, Artificial Intelligence and Statistical Experimental Design For the Modelling and Optimization of Methylene Blue and CD (II) Removal from a Binary Aqueous Solution By Natural Walnut Carbon. Royal Society of Chemistry, 19 (18), 11299-11317 https://doi.org/10.1039/c6cp08437k
- Mgbemena, C., Mgbemena, C.E., Etebenumeh, G., & Ashiedu, F. (2016). Effect of turning parameters on metal removal and tool wear rates of AISI 1018 low carbon steel. Nigerian Journal of Technology, 35(4), 847-854.
- Mohsen, S., & Mohammed, A. (2022). A Review of the Recent Development in Machining Parameter Optimization. Jordan Journal of Mechanical and Industrial Engineering, 16 (2), 205-223.
- Mourabet, M.E., Rhilassi, A., Bennani-Ziatni, M. & Taitai, A. (2014). Comparative Study of artificial neural network and response surface methodology for modelling and optimization the adsorption capacity of fluoride onto apatitic tricalcium phosphate. Universal Journal of Applied Mathematics, 2 (2), 84–91. https://doi.org/10.13189/ujam.2014.020202

- Nazerian, M., Kamyabb, M., Shamsianb, M., Dahmardehb, M. & Kooshaa, M. (2018). Comparison of response surfacemethodology (RSM) and artificial neural networks (ANN) towards efficient optimization of flexural properties of gypsum-bonded fiberboards. CERNE 24 (1), 35–47.
- Oguanobi, N.C., Onu, C.E. & Onukwuli, O.D. (2019). Adsorption of a dye (crystal violet) on an acid modified nonconventional adsorbent. Journal of Chemical Technology and Metallurgy, 54 (1), 95-110
- Ohale, P.E., Uzoh, C.F., & Onukwuli, O.D. (2017). Optimal factor evaluation for the dissolution of alumina from azaraegbelu clay in acid solution using RSM and ANN comparative analysis. South African Journal of Chemical Engineering, 24, 43–54. https://doi.org/10.1016/j.sajce.2017.06.003
- Okpe, E.C., Asadu, C.O. & Onu, C.E. (2018). Statistical analysis for orange G adsorption using kola nut shell activated carbon, Journal of the Chinese Advanced Materials Society, 6(4), 605-619, https://doi.org/10.1080/22243682.2018.1534607
- Okwu, M.O. & Adetunji, O. (2018). A comparative study of artificial neural network (ANN) and adaptive neuro-fuzzy inference system (ANFIS) models in distribution system with nondeterministic inputs. International Journal of Engineering Business Management, 10, 1–17. https://doi.org/10.1177/1847979018768421
- Olayode, I.O.; Tartibu, L.K. & Alex, F.J. (2023). Comparative Study Analysis of ANFIS and ANFIS-GA Models on Flow of Vehicles at Road Intersections. Applied Sciences, 13(744), 1-22. https://doi.org/10.3390/app13020744
- Onu, C.E., Igbokwe, P.K., Nwabanne, J.T., Nwanjinka, O.C. & Ohale, P.E. (2020). Evaluation of optimization techniques in predicting optimum moisture content reduction in drying potato slices. Artificial Intelligence in Agriculture, 4, 39–47. https://doi.org/10.1016/j.aiia.2020.04.001
- Onu, C.E., Nwabanne, J.T., Ohale, P.E. & Asadu, C.O. (2021). Comparative analysis of RSM, ANN, and ANFIS and the mechanistic modelling in eriochrome black-T dye adsorption using modified clay. South African Journal of Chemical Engineering, 36, 24-42. https://doi.org/10.1016/j.sajce.2020.12.003
- Parthasarathi, N. L., Dhinakaran, V., Duraisami, D., Utpal, B., Ravichandran, M., L. Natrayan, L. & Wubishet, D. M. (2022). Influence of End Milling Process Variables on Material Removal Rate and Surface Roughness of DirectMetal Laser Sintered Inconel 718 Plate. Advances in Materials Science and Engineering, 2022(9101820), 1-14. https://doi.org/10.1155/2022/9101820
- Sada, S.O. (2021). Improving the predictive accuracy of artificial neural networks (ANN) approach in a mild steel turning operation. Journal of Advanced Manufacturing Technology, 112 2389–2398
- Sada, S., & Ikpeseni S.C. (2021). Evaluation of ANN and ANFIS modelling ability in the prediction of AISI 1050 steel machining performance. Heliyon 7(2), 1-9. https://doi.org/10.1016/j.heliyon.2021.e06136
- Salimiasi, A. & Özdemir, A. (2016). Analysing the performance of artificial neural network (ANN)-, fuzzy logic (FL) and least square (LS)-based models for online tool condition monitoring. International Journal of Advanced Manufacturing Technology, 87, 1145–1158. https://doi.org/10.1007/s00170-016-8548-x
- Sahu, J.N., Acharya, J. & Meikap, B.C. (2010). Optimization of production conditions for activated carbons from tamarind wood by zinc chloride using response surface methodology. Bioresources Technology, 101 (6), 1974–1982. https://doi.org/10.1016/j.biortech.2009.10.031
- Sandeep, K., Dhanabalan, S., & Narayanan, C. S. (2019). Application of ANFIS and GRA for multi-objective optimization of optimal wire-EDM parameters while machining Ti–6Al–4 V alloy. Springer Nature Applied Sciences, 1(298), 1-12. https://doi.org/10.1007/s42452-019-0195-z
- Shagwira, H., Mbuya, T.O.,, Mwema, F.M., Herzog, M. & Akinlabi, E.T. (2021). Taguchi Optimization of Surface Roughness and Material Removal Rate in CNC Milling of Polypropylene + 5wt.% Quarry Dust Composites. Materials Science and Engineering, 1107 (012040), 1-10. https://doi.org/10.1088/1757-899X/1107/1/012040
- Shrikrishna, N., Gururaj, B. & Argha, D. (2018). Measurement and analysis of cutting force and product surface quality during end-milling of thin-wall components. Measurement, 121, 190-204, https://doi.org/10.1016/j.measurement.2018.02.015
- Shukry, H., Aghdeab, I., Adil, S. J., Mohammed, S. J., & Baqer, A. A. (2018). ANFIS optimization of cutting parameters for MRR in turning processes. Association of Arab Universities Journal of Engineering Sciences, 25(4), 74-84
- Sidda, R.B., Kumar, J.S. & Reddy, K.V.K. (2011). Optimization of surface roughness in CNC end milling using response surface methodology and genetic algorithm. International Journal of Engineering, Science and Technology, 3(8), 102-109
- Singh, N.K., Singh, Y. & Kumar, S. (2019). Comparative study of statistical and soft computing-based predictive models for material removal rate and surface roughness during helium-assisted EDM of D3 die steel. SN Applied Sciences, 1(529). https://doi.org/10.1007/s42452-019-0545-x
- Taran, M. & Aghaie, E. (2015). Designing and optimization of separation process of iron impurities from kaolin by oxalic acid in bench-scale stirred-tank reactor. Applied clay science, 107, 109-116. https://doi.org/10.1016/j.clay.2015.01.010.

- Thike, P.H., Zhao, Z. & Shi, P. (2020). Significance of artificial neural network analytical models in materials' performance prediction. Bulletin of Material Science, 43(211). https://doi.org/10.1007/s12034-020-02154-y
- Wickramarachchi, C.T., Rogers, T.J., Leahy, W. & Cross, E.J. (2021). Predicting Tool Wear Using Linear Response Surface Methodology and Gaussian Process Regression. Topics in Modal Analysis & Testing, 8, 283-286. https://doi.org/10.1007/978-3-030-47717-2_29
- Ying, L.C. & Pan, M.C. (2008). Using adaptive network based fuzzy inference system to forecast regional electricity loads, Energy Conversion Management, 49, 205–211
- Zhang, W., Zhang, L. & Wang, S. (2019). Optimization of machining parameters of 2.25Cr1Mo0.25 V steel based on response surface method and genetic algorithm. International Journal on Interactive Design Manufacturing, 13, 809–819. https://doi.org/10.1007/s12008-018-00525-8

Declarations

Funding: No specific funding was received for this work.
Potential competing interests: No potential competing interests to declare.